

SANDIA REPORT

SAND91-2322 • UC-523

Unlimited Release

Printed June 1992

Gas Blowthrough and Flow Quality Correlations for Use in the Analysis of High Pressure Melt Ejection (HPME) Events

Martin Pilch, Richard O. Griffith

Prepared by
Sandia National Laboratories
Albuquerque, New Mexico 87185 and Livermore, California 94550
for the United States Department of Energy
under Contract DE-AC04-76DP00789



SAND91-2322
0002
UNCLASSIFIED

06/92
56P

STAC

Issued by Sandia National Laboratories, operated for the United States Department of Energy by Sandia Corporation.

NOTICE: This report was prepared as an account of work sponsored by an agency of the United States Government. Neither the United States Government nor any agency thereof, nor any of their employees, nor any of their contractors, subcontractors, or their employees, makes any warranty, express or implied, or assumes any legal liability or responsibility for the accuracy, completeness, or usefulness of any information, apparatus, product, or process disclosed, or represents that its use would not infringe privately owned rights. Reference herein to any specific commercial product, process, or service by trade name, trademark, manufacturer, or otherwise, does not necessarily constitute or imply its endorsement, recommendation, or favoring by the United States Government, any agency thereof or any of their contractors or subcontractors. The views and opinions expressed herein do not necessarily state or reflect those of the United States Government, any agency thereof or any of their contractors.

Printed in the United States of America. This report has been reproduced directly from the best available copy.

Available to DOE and DOE contractors from
Office of Scientific and Technical Information
PO Box 62
Oak Ridge, TN 37831

Prices available from (615) 576-8401, FTS 626-8401

Available to the public from
National Technical Information Service
US Department of Commerce
5285 Port Royal Rd
Springfield, VA 22161

NTIS price codes
Printed copy: A03
Microfiche copy: A01

SAND91-2322
Unlimited Release
Published June 1992

Distribution
Category UC-523

**GAS BLOWTHROUGH AND FLOW QUALITY CORRELATIONS
FOR USE IN THE ANALYSIS OF
HIGH PRESSURE MELT EJECTION (HPME) EVENTS**

Martin Pilch
Severe Accident Phenomenology
Richard O. Griffith
Containment Modeling
Sandia National Laboratories
Albuquerque, New Mexico 87185

ABSTRACT

A number of correlations describing the advent of gas blowthrough and the subsequent exit quality were collected and examined. A simple scaling analysis was applied to these correlations to identify important nondimensional groups, and the range of values for these dimensionless groups at nuclear power plant (NPP) and experimental scales were used to examine the applicability of the correlations at different scales. The performance of each of the correlations was also assessed over a typical parameter range for NPP and experimental conditions. The Gluck correlation for the onset of gas blowthrough is recommended for high pressure melt ejection analyses. A new model is developed for predicting the two-phase flow quality following the onset of gas blowthrough. Uncertainty estimates for the blowthrough correlation and the flow quality correlation are quantified.

CONTENTS

<u>Section</u>	<u>Page</u>
1.0 INTRODUCTION	1
2.0 GAS BLOWTHROUGH	2
2.1 Scaling Analysis of Gas Blowthrough	2
2.2 Correlations for the Onset of Gas Blowthrough	5
2.3 Recommended Blowthrough Correlation	6
2.4 Uncertainty in the Gas Blowthrough Correlation	7
3.0 FLOW QUALITY	18
3.1 Scaling Analysis of Flow Quality	18
3.2 Correlations of Flow Quality	20
3.3 Development of a Recommended Flow Quality Model for DCH Analyses	21
3.4 Uncertainty in the Gas Quality Model	25
4.0 CONCLUSIONS AND RECOMMENDATIONS	32
5.0 REFERENCES	33

FIGURES

<u>Figure</u>		<u>Page</u>
1.	Gas Blowthrough Phenomena	14
2.	Correlation Comparison for the Onset of Gas Blowthrough	15
3.	The Effect of Tank Diameter on the Onset of Gas Blowthrough	16
4.	Contribution of Competitive Correlations to the Uncertainty in Applying a Recommended Correlation	17
5.	Model Comparison with Available Correlations Developed for Horizontal Pipes	28
6.	Predicted Effect of System Scale on Gas Quality	29
7.	Predicted Effect of Tank/Hole Diameter Ratio at NPP Scale on Gas Quality	30

TABLES

<u>Table</u>	<u>Page</u>
1. Typical Values of Dimensionless Parameters	10
2. Descriptions of Gas Blowthrough Correlations	11
3. Applicability of Gluck Correlation to DCH Analyses at NPP and Experiment Scales	12
4. Parameters for Estimating the Overall Uncertainty in Applying the Gluck Correlation to DCH Analyses	13
5. Scaling Dependencies for Available Flow Quality Correlations with Downward Facing Holes	26
6. Parameters for Evaluating the Gas Quality Correlation for Hemispherical Tanks at Different Scales	27
7. Parameters for Estimating the Overall Uncertainty in Applying Gas Quality Correlations for Horizontal Pipes	31

NOMENCLATURE

A_b	=	area of hole
A_1	=	area of liquid exiting hole
Bo	=	Bond Number, $Bo = \frac{\rho g D^2}{\sigma}$
C_d	=	discharge coefficient at hole
$C_{1,2}$	=	constant
d	=	hole diameter
d_i	=	instantaneous diameter characterizing liquid flow following blowthrough
d_g	=	instantaneous diameter of the gas core
D	=	tank diameter
Fr	=	Froude Number, $Fr = \frac{u}{\sqrt{gd}}$
g	=	gravitational acceleration
h	=	height of liquid above hole
h_b	=	height of liquid above hole at gas blowthrough
MW_g	=	molecular weight of the gas
P_1	=	upstream pressure
P_2	=	downstream pressure
\dot{Q}	=	volumetric flow rate
R_u	=	gas constant
Re	=	Reynolds Number, $Re = \frac{\rho u D}{\mu}$
T_b	=	gas temperature
u	=	liquid velocity at exit
W_{sg}	=	mass flow rate of single phase gas
W_{sl}	=	mass flow rate of single phase liquid
We	=	Weber Number, $We = \frac{\rho d u^2}{\sigma}$
X_g	=	gas exit quality
X_l	=	liquid exit quality

NOMENCLATURE concluded

Greek Symbols

α_g	=	gas void fraction
α_l	=	liquid void fraction
μ	=	liquid viscosity
ρ	=	liquid density
ρ_g	=	gas density
ΔP	=	difference between the upstream and downstream pressures
γ	=	isentropic gas expansion coefficient
σ	=	liquid surface tension

1.0 INTRODUCTION

Direct containment heating (DCH) can occur in a nuclear power plant (NPP) if, as a result of a core melt accident, molten material accumulates on the lower head of the reactor pressure vessel (RPV) causing it to fail by thermally induced rupture or by expulsion of an incore instrument guide tube. DCH is only of interest if the RPV failure occurs while the reactor coolant system (RCS) is still at elevated pressure; in which case, lower head failure initiates forcible ejection of melt into the reactor cavity. These processes have been termed high pressure melt ejection (HPME).

Blowdown gas from the RCS during an NPP accident adds both mass and energy to the containment atmosphere. Some portions of the molten material that is ejected into the reactor cavity can be entrained, fragmented, and dispersed into the containment atmosphere. Debris dispersed from the reactor cavity can rapidly liberate its thermal energy to the containment atmosphere. The metallic components of the dispersed material can oxidize with steam liberating both energy and hydrogen. These processes will heat the containment atmosphere, possibly to the point at which steam can no longer inert the combustion of hydrogen. The resultant DCH can lead to early failure of the reactor containment building (RCB) by overpressurization.

Large scale experiments (1:10 linear scale) are being conducted at Sandia National Laboratories (SNL) [Allen et al., 1991a,b,c; Allen et al., 1992a,b,c] to investigate DCH phenomena. A detailed scaling analysis¹ supports this experiment program. The system level computer code, CONTAIN [Murata et al., 1990], is being used to analyze experiments [Allen et al., 1992c] and to perform predictions of reactor response to DCH events [Williams et al., 1987; Williams and Louie, 1988]. The assessment of models and correlations performed in this document supports both the scaling activities and the detailed modeling activities.

Gas blowthrough and two-phase flow following the onset of gas blowthrough have been identified [NRC 1991] as potentially important processes that could impact DCH loads. The purpose of this document is

1. to identify candidate models and correlations in the literature,
2. to assess the applicability of the models and correlations to experiment and reactor analyses,
3. to quantify uncertainties associated with the recommended model or correlation,
4. to make recommendations for current modeling activities and future research.

¹ Marty Pilch and Michael D. Allen, A Scaling Methodology for Direct Containment Heating with Application to the Design and Specification of an Experiment Program for Resolving DCH Issues, to be published, SAND91-2784, Sandia National Laboratories, Albuquerque, NM.

2.0 GAS BLOWTHROUGH

The pressurized ejection of liquid from a tank progresses through three possible phases: single-phase liquid discharge, two-phase gas/liquid discharge, and single-phase gas discharge. Single-phase discharge progresses until, at some critical liquid level, a funnel-like depression forms over the outlet hole as depicted in Figure 1. This is termed gas blowthrough. This section addresses the critical liquid level at which gas blowthrough is initiated.

2.1 Scaling Analysis of Gas Blowthrough

The critical liquid level at the onset of blowthrough is postulated to be a function of the following set of variables

$$h_b = f \{u; u_t; g; \rho_g; \rho; \mu; \sigma; d; D; \text{geometry}\} \quad (1)$$

where

h_b	=	critical liquid level at the onset of blowthrough,
u	=	velocity of liquid out the hole,
u_t	=	tangential velocity characterizing swirl near the hole,
g	=	acceleration due to gravity,
ρ_g	=	gas density,
ρ	=	liquid density,
μ	=	liquid viscosity,
σ	=	liquid surface tension,
d	=	diameter of the orifice through which the liquid flows, and
D	=	characteristic diameter of the tank.

This list is thought to include all variables known or postulated by the relevant literature to influence the onset of blowthrough. Note that geometry, which refers to vessel shape and orientation (e.g., horizontal pipes versus upright cylinders), is also postulated to influence blowthrough. The implied assumption in formulating this list is that the onset of gas blowthrough is dominated by hydrodynamic phenomena that are not significantly influenced by the presence of solid particles, heat transfer, and chemical reactions. All these phenomena can exist to some degree in a reactor application; however, the authors have subjectively judged these concerns to be second order effects.

Application of the Buckingham Pi Theorem renders the original set nondimensional,

$$\frac{h_b}{d} = f \left\{ Fr, Re, Bo, \frac{\rho_g}{\rho}, \frac{d}{D}, N_T; \text{geometry} \right\} \quad (2)$$

where

$$Fr = \frac{u}{\sqrt{gd}} \quad \text{Froude number} \quad , \quad (3)$$

$$Re = \frac{\rho u D}{\mu} \quad \text{Reynolds number} \quad , \quad (4)$$

$$Bo = \frac{\rho g D^2}{\sigma} \quad \text{Bond number} \quad , \quad (5)$$

$$N_r = \frac{u_i}{u} \quad \text{circulation number} \quad . \quad (6)$$

This set of scaling groups is not unique because the Buckingham Pi Theorem, as a corollary, states that any group can be replaced by products or ratios of other groups; therefore, caution must be exercised in comparing the available models and correlations.

Representative values for the dimensionless parameters given in Equation 2 are presented in Table 1 for typical NPP and experiment conditions. The NPP values correspond to a pump seal LOCA ($\Delta P=6.2$ MPa) induced by a station blackout accident in the Zion nuclear power plant. Approximately 50 Mt of molten core material is assumed to be on the lower head of the RPV when vessel failure occurs, which is assumed to be by gross rupture forming a large hole ($D=1.0$ m) or by tube ejection followed by ablation forming a smaller hole ($D=0.35$ m). The 1:10 scale values represent typical conditions for DCH experiments conducted at the SNL Surtsey test facility [Allen et al., 1991a,b,c; Allen et al., 1992a,b,c]. The 1:40 scale values represent typical conditions for DCH experiments to be conducted at Argonne National Laboratory (ANL). The SNL and ANL experiments are guided by the NPP application for Zion or similar conditions for the Surry NPP.

The Froude number, Fr , characterizes the rate at which disturbances are convected through the outlet compared to the rate at which surface disturbances propagate towards the outlet. A systematic elimination of all but one of the remaining scaling groups will leave the Froude number as the dominant physical parameter controlling the onset of gas blowthrough.

The Reynolds number, Re , characterizes viscous effects. Gluck et al. [1966a,b] found no appreciable effect on the gas blowthrough height for $10^2 < Re < 10^5$. Gluck et al. [1966a,b] also stated that the Reynolds numbers would have to lie well below the given lower bound to produce appreciable viscosity effects on the gas blowthrough height. Table 1 shows that the Reynolds number for DCH applications far exceeds the value where viscosity effects might be important; therefore, the Reynolds number can be eliminated from the set of essential scaling groups.

The Bond number, Bo , characterizes surface tension effects. The Weber number, We ,

$$We = \frac{\rho u^2 d}{\sigma} \quad (7)$$

has also been used to characterize surface tension effects in some applications [Easton and Catton, 1970]; however, the Weber number is not an independent group because it can be formed from the product or ratio of other groups found in Equation 2. Investigations on the effect of the Bond number [Gluck et al., 1966a,b] revealed no significant effects for $Bo > 60$. In a later investigation, Gluck et al. [1966a,b] concluded that surface tension effects were probably negligible for $Bo > 5$. Gluck et al. [1966a,b] also stated that the Bond number would have to lie well below the given lower bound to produce appreciable surface tension effects on the gas blowthrough height. Table 1 shows that the Bond number for DCH applications far exceeds the value where surface tension effects might be important; therefore, the Bond number can be eliminated from the set of essential scaling groups.

Swirl or vortex formation generally accelerates the onset of blowthrough (i.e., blowthrough occurs at a greater depth h_b/d , [Riemann and Khan 1983, Smoglie and Riemann 1986]). The circulation number, N_r , characterizes swirl effects as the liquid approaches the outlet. Daggett and Keulegan [1974] found that swirl effects were negligible for $N_r < 0.1$. Daggett's experiments employed spinning tanks with liquid withdrawal from a hole in the bottom. Therefore, the application of this criteria is ambiguous to applications with crossflow or other potential sources of vorticity. In experiment and reactor geometries, there is no crossflow at the hole and the effects of swirl are expected to be negligible for DCH analyses. This report intentionally focuses on those models and correlations for which swirl effects are negligible; therefore, the circulation number can be eliminated from the list of essential scaling groups.

The density ratio, ρ_g/ρ , usually characterizes buoyancy effects, an effect studied by Lubin and Springer [1967]. The reported influence of the density ratio on gas blowthrough is given by

$$h_b \sim \left(\frac{1}{1 - \frac{\rho_g}{\rho}} \right)^{0.2} \quad (8)$$

This expression was developed for density ratios ranging from near zero to near unity. The latter was achieved by substituting light liquids for the gas in the experiments. The Lubin and Springer expression shows that blowthrough is only influenced by the density ratio when ρ_g/ρ is comparable to unity. Table 1 shows that this certainly is not the case in DCH applications; therefore, the density ratio can be eliminated from the list of essential scaling groups.

Gluck et al. [1966a,b] studied the effect of tank diameter on gas blowthrough, characterized by the ratio D/d , and found that the tank diameter significantly suppressed the onset of blowthrough when $D/d < 15$. Table 1 shows that DCH applications all fall in this range; therefore, the ratio D/d remains essential for scaling blowthrough phenomena in DCH applications. The effect of tank diameter will be discussed more fully in Section 2.4.

The geometry of interest for NPP applications is an upright cylinder where all the liquid is expected to reside in a hemispherical bottom. There is a notable scarcity of data for hemispherical geometry; consequently, data for other geometries will be considered as part of the assessment. A more detailed discussion of geometry will be delayed until Section 2.4; so for now, geometry will remain an essential element of the scaling analysis.

The list of scaling groups characterizing the onset of gas blowthrough in DCH applications reduces to

$$\frac{h_b}{d} = f \left\{ Fr, \frac{d}{D}; \text{geometry} \right\} \quad (9)$$

when only the essential elements are retained. This reduced set of scaling groups forms the basis for assessing the applicability of available correlations to DCH analyses at experiment and reactor scales.

The scaling analysis shows that blowthrough phenomena are not preserved by strict geometric scaling of experiments because the Froude number has an embedded length scale that is not ratioed by any other physical length associated with the hardware. The implication is that blowthrough is expected earlier (a greater h_b/d) in small scale experiments. However, when evaluating typical DCH experiments is often found that the fraction of the melt mass remaining in the vessel at the onset of blowthrough may not differ significantly from what would be expected at reactor scale. Two reasons for this apparent insensitivity can be identified. First, the dependence of h_b/d on scale, d , is weak, being only to the 1/5th power as discussed below. Secondly, strict geometric scaling of the liquid volumes is not usually employed in the experiments. Consequently the initial fluid depth (h^0/d) is somewhat larger in experiments than at reactor scale, and this partially compensates for the somewhat earlier blowthrough. The exact implications of scale distortions must be carefully evaluated for each application.

2.2 Correlations for the Onset of Gas Blowthrough

The most common form of the blowthrough correlation is given by

$$\frac{h_b}{d} = C_1 Fr^{C_2} \quad (10)$$

Although the same basic form has been used by many researchers, the reported values for the constants C_1 and C_2 tend to differ. Table 2 summarizes reported values for these constants and indicates conditions under which each correlation applies. The constants have been separated into two groups depending upon whether a vortex exists at the onset of gas blowthrough. In all cases listed as vortex free, the authors explicitly state (based on visual observation) that vortex motion did not exist. Smoglie and Reimann [1986] and Schrock et al. [1985] explicitly state that vortex motion was observed. Anderson and Owca [1985] and Maciaszek and Memponteil [1986] inferred the onset of blowthrough from pressure measurements, but neither made visual observations to confirm the absence (or existence) of vortices. Anderson and Owca [1985] assumed that they had no vortex motion because Smoglie [1984] stated that small velocities past the branch results in vortex free flow behavior. Yonomoto and Tasaka [1988] state that vortex

motion was observed, but they considered it insignificant because their results were consistent with Anderson and Owca [1985] and Maciaszek and Memponteil [1986] who assumed that they were vortex free. With these considerations in mind, Table 2 shows that the constants are consistent amongst researchers provided vortex free flow is properly distinguished from vortex flow.

A significant subset of these correlations can be written in the form

$$\left(\frac{\pi h_b^{2.5} \sqrt{g}}{4 \dot{Q}} \right)^{0.4} = C_1, \quad (11)$$

which is valid whenever $C_2 = 0.4$. This result says that blowthrough is governed by a critical value of a single scaling group and that the depth for blowthrough is determined solely by the volume flow rate, \dot{Q} , (assuming gravity is not a control variable).

Schrock et al. [1986] proposed a far more complicated expression to account for viscosity and surface tension effects:

$$Fr \frac{d^2 \sigma}{g \Delta \rho} \frac{1}{\sqrt{\mu_i \rho_i^{-0.5} \sigma^{-0.75} (g \Delta \rho)^{0.25}}} \sqrt{\frac{\rho_i}{\Delta \rho}} = 19.4 \left(\frac{d \left(\frac{h_b}{d} \right)}{\sqrt{\frac{\sigma}{g \Delta \rho}}} \right)^{2.2}. \quad (12)$$

This correlation was developed for $10 < D/d < 25$ and $10 < Fr < 100$. The geometry corresponds to a horizontal pipe with a downward facing hole.

Gluck et al. [1966a,b] proposed yet another form for the blowthrough correlation,

$$\frac{h_b}{d} = 0.43 \frac{D}{d} \tanh \left(Fr^{1/2} \frac{d}{D} \right) \quad (13)$$

This correlation is valid for $3.2 < D/d < 20$ and $0.32 < Fr < 320$. The correlation was developed for upright cylinders with both flat and hemispherical bottoms. As such, the Gluck correlation is the only correlation explicitly applicable to the hemispherical geometries expected in reactor applications. The Gluck correlation limits to Equation 10, with $C_1=0.43$ and $C_2=0.5$, in the limit when D/d is very large.

2.3 Recommended Blowthrough Correlation

Figure 2 compares the candidate correlations for the onset of gas blowthrough for a range Froude numbers representative of both experiment and reactor conditions. The Gluck et al. [1966a,b] correlation is plotted assuming that the d/D ratio approaches zero. The correlations are banded into two groups. In the upper group, all the correlations were developed for horizontal pipes with vortex motion. Three of the five correlations in the lower group were developed for

upright cylinders, but all five were vortex free. This demonstrates that the presence of vortices has a significant effect on gas blowthrough. It does not appear that geometry (horizontal pipe, vertical cylinder, or hemisphere) has a significant effect on blowthrough behavior. However, correlations for vortex free flow are more appropriate for reactor applications because strong sources of circulation (such as cross flow at a tee) are not expected in the molten material pooled-up on the lower head of the reactor pressure vessel during HPME. Only the Gluck correlation, which is in the lower group of vortex free correlations, is explicitly applicable to both the flat- and hemispherical-bottomed vessels typical of experiment and NPP applications.

Only the Gluck correlation embodies the effects of tank diameter, which the scaling analysis identified as potentially important for both experiment and reactor analyses. Figure 3 plots the Gluck correlation for a range of D/d representative of DCH analyses. The ratio, D/d , has a significant effect on gas blowthrough for surprisingly large values of D/d . Failure of all other candidate correlations to account for this effect renders them undesirable for DCH analyses.

Table 3 summarizes the applicability of the Gluck correlation to DCH analyses at both NPP and experiment scales. The data base fully covers the range of essential parameters necessary for DCH analyses. In summary, the Gluck correlation is recommended for DCH analyses because

1. it explicitly applies to the geometry of interest (i.e., flat and hemispherical bottomed cylinders),
2. it explicitly shows the effects of tank diameter, and
3. the data base spans the range of Fr and D/d values of interest to DCH analyses.

2.4 Uncertainty in the Gas Blowthrough Correlation

Quantification of the uncertainty in DCH events requires quantification of the contributing phenomenologies, in this case, the onset of gas blowthrough. Two sources of uncertainty in applying a recommended correlation will be considered: data scatter for the recommended correlation and differences between the recommended and competitive correlations. This section develops a quick and easy method for combining these uncertainties. Uncertainties associated with a potentially incomplete understanding of the blowthrough process are not considered here.

Estimates of total uncertainty follow from Figure 4. For now, the development assumes that only two correlations are available: correlation A, the recommended correlation, and correlation B, the competitive correlation. The results will be generalized later to accommodate any number of competitive correlations. Correlation A comes from a data base containing N_A data points, while correlation B comes from a database containing N_B independent data points. The total uncertainty ($\sigma_{A,B}$) could be obtained by computing the relative root-mean-square (RMS) error of all data points from all data sets about the recommended correlation,

$$\sigma_{A,B}^2 = \frac{\sum_{i=1,N_A} \left[\frac{f(a_i) - f_A(a_i)}{f_A(a_i)} \right]^2 + \sum_{j=1,N_B} \left[\frac{f(b_j) - f_A(b_j)}{f_A(b_j)} \right]^2}{N_A + N_B}, \quad (14)$$

where

$f(a_i), f(b_j)$ = the y values of the data points (measurements) located at a_i and b_j , respectively with the first belonging to data set "A" and the second belonging to data set B, and
 $f_A(a_i), f_A(b_j)$ = the y values computed from the recommended correlation for the data points.

Computing the total uncertainty from this expression is not practical in most situations because the data usually is not available in a convenient form.

Expanding the term under the second summation leads to a more convenient method for estimating the combined uncertainty in applying the recommended correlation. Performing the indicated expansion

$$\sum_{j=1,N_B} [f(b_j) - f_A(b_j)]^2 = \sum_{j=1,N_B} \left[(f(b_j) - f_B(b_j)) + (f_B(b_j) - f_A(b_j)) \right]^2, \quad (15)$$

yields

$$\begin{aligned} \sum_{j=1,N_B} [f(b_j) - f_A(b_j)]^2 &= \sum_{j=1,N_B} [f(b_j) - f_B(b_j)]^2 + \sum_{j=1,N_B} [f_B(b_j) - f_A(b_j)]^2 \\ &+ \sum_{j=1,N_B} 2 [f(b_j) - f_B(b_j)] [f_B(b_j) - f_A(b_j)] \end{aligned} \quad (16)$$

when the square is completed. The last summation on the right-hand-side (RHS) tends to zero because $f(b_j) - f_B(b_j)$ represents scatter of the data set "B" about its own correlation line. With this substitution, the total uncertainty takes on the form

$$\sigma_{A,B}^2 = \frac{N_A}{N_A + N_B} \sigma_A^2 + \frac{N_B}{N_A + N_B} (\delta_{A,B}^2 + \sigma_B^2), \quad (17)$$

where

σ_A, σ_B = reported standard deviations of the data sets "A" and "B" about their respective correlations, and
 $\delta_{A,B}$ = mean RMS offset between the correlations.

The latter can be estimated from comparative plots of the correlations over the parameter range of interest.

This result can be generalized to the case where "Nk" competitive correlations are available, one of which is selected as the recommended correlation,

$$\sigma^2 = \sum_{k=1, N_k} f_{N_k} (\delta_k^2 + \sigma_k^2) , \quad (18)$$

where the weights

$$f_{N_k} = \frac{N_k}{\sum_{m=1, N_m} N_m} \quad (19)$$

represent the fractional number of all data points from all correlation sets that form the basis for correlation "k".

Application of this procedure to an uncertainty analysis of gas blowthrough correlations can be performed with the information supplied in Table 4. The Gluck et al. [1966a,b] correlation is recommended for blowthrough analyses of DCH events, while the Lubin and Springer [1967] and Reimann and Khan [1983] supply the competitive correlations. The Smoglie and Reimann [1986] and Crowley and Rothe [1981] correlations were not considered because insufficient information was presented in the papers. The offset for the correlations is estimated from the maximum difference in the two correlations with the Gluck correlation evaluated for an infinitely wide tank, which is the range of overlap in the three data bases. The estimated total uncertainty in applying the Gluck correlation to DCH analyses is $\pm 20\%$, which is less than the scatter in Gluck's original data. This is possible because the Lubin and Springer data set is much more tightly banded and falls within the scatter of Gluck's data. However, this reduced uncertainty is justified only for large D/d values. The more conservative value of $\pm 25\%$ (as reported by Gluck et al.) is recommended here because it is applicable over the entire parameter range of interest to the applications.

Table 1.
Typical Values of Dimensionless Parameters

Parameter	NPP Scale 1:1	Surtsey Scale 1:10	ANL Scale 1:40
Fr	7.7 - 12.9	34.0 - 54.6	108.1
Re	$10^7 - 10^8$	$10^6 - 10^7$	$10^5 - 10^6$
Bo	$10^5 - 10^6$	6.3×10^3	400
ρ_g/ρ	0.0035	0.0062	0.0062
D/d	4.4 - 12.6	4.4 - 11.4	11.4

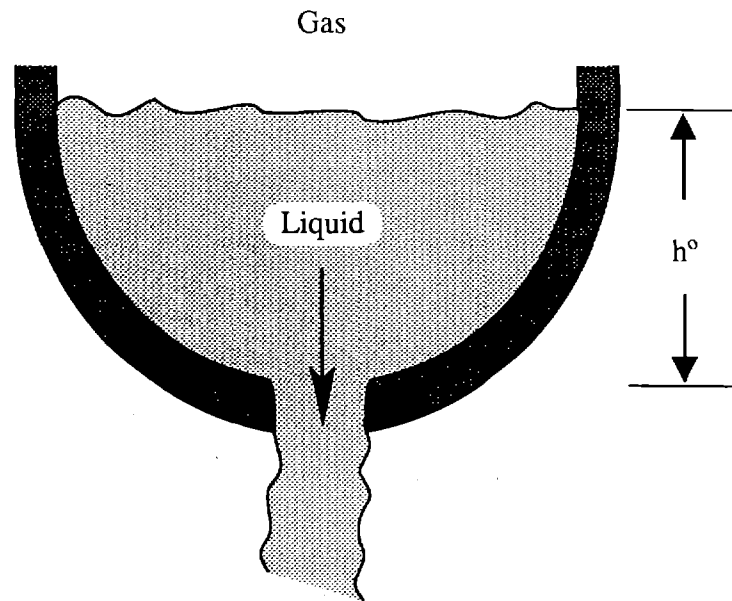
Table 2. Descriptions of Gas Blowthrough Correlations							
Reference	Vortex Free		Vortex		Fr Range	D/d Range	Geometry
	C ₁	C ₂	C ₁	C ₂			
Yonomoto and Tasaka 1988			0.91	0.4	4.5 - 63.9	9.1 - 20	Horizontal Pipe
Smogleie and Reimann 1986	0.62	0.4	1.03	0.4	2.7 - 86.4	10.3 - 33.3	Horizontal Pipe
Schrock et al. 1985			0.82 0.65	0.5 0.5	10 - 100 10 - 100	10.2 - 25	Horizontal Pipe
Anderson and Owca 1985			0.91	0.4			Horizontal Pipe
Maciaszek and Mernponteil 1986			0.91	0.4			Horizontal Pipe
Reimann and Khan 1983	0.62	0.4			2 - 60	6.8 - 33.3	Horizontal Pipe
Crowley and Rothe 1981	0.62	0.4			1.2 - 41.3	12.0	Horizontal Pipe
Lubin and Hurwitz 1966	0.62	0.4			0.1 - 14		Cylinder
Lubin and Springer 1967	0.63	0.4			0.2 - 100	9.1 - 71.4	Cylinder
Gluck et al. 1966a,b	0.43	0.5			0.316 - 316	3.2 - 20	Cylinder Hemisphere

**Table 3.
 Applicability of Gluck Correlation
 to DCH Analyses at NPP and Experiment Scales**

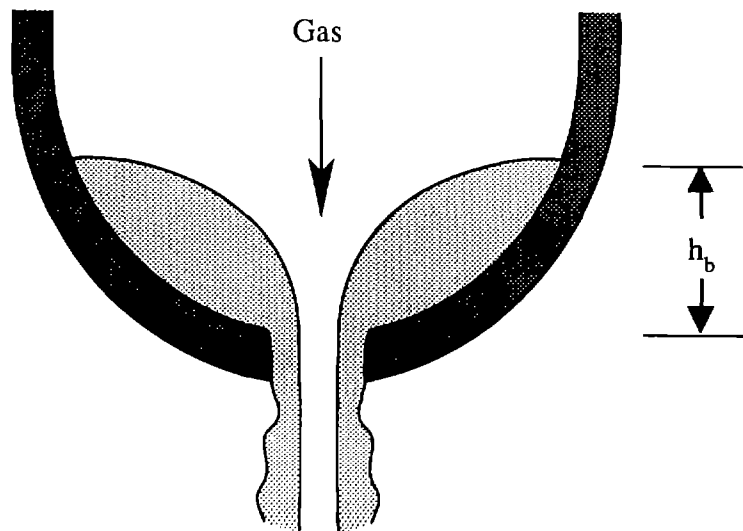
Scaling Group	Data Base	NPP Scale 1:1	Surtsey Scale 1:10	ANL Scale 1:40
Fr	0.32 - 320	7.7 - 12.9	34.0 - 54.6	108.1
D/d	3.2 - 20	4.4 - 11.4	4.4 - 11.4	4.4 - 11.4
Geometry	Flat and Hemispherical Bottomed Cylinder	Hemispherical Bottomed Cylinder	Flat and Hemispherical Bottomed Cylinder	Hemispherical Bottomed Cylinder

Table 4.
Parameters for Estimating the Overall Uncertainty
in Applying the Gluck Correlation to DCH Analyses

Reference	N Data Points	σ RMS Scatter	δ RMS Offset
Gluck et al. 1966a,b	61	0.25	0
Lubin and Springer 1967	33	0.04	0.05
Reimann and Khan 1983	32	0.20	0.05



Single Phase
Discharge



Onset of Blowthrough
and Two-phase
Discharge

Figure 1. Gas Blowthrough Phenomena

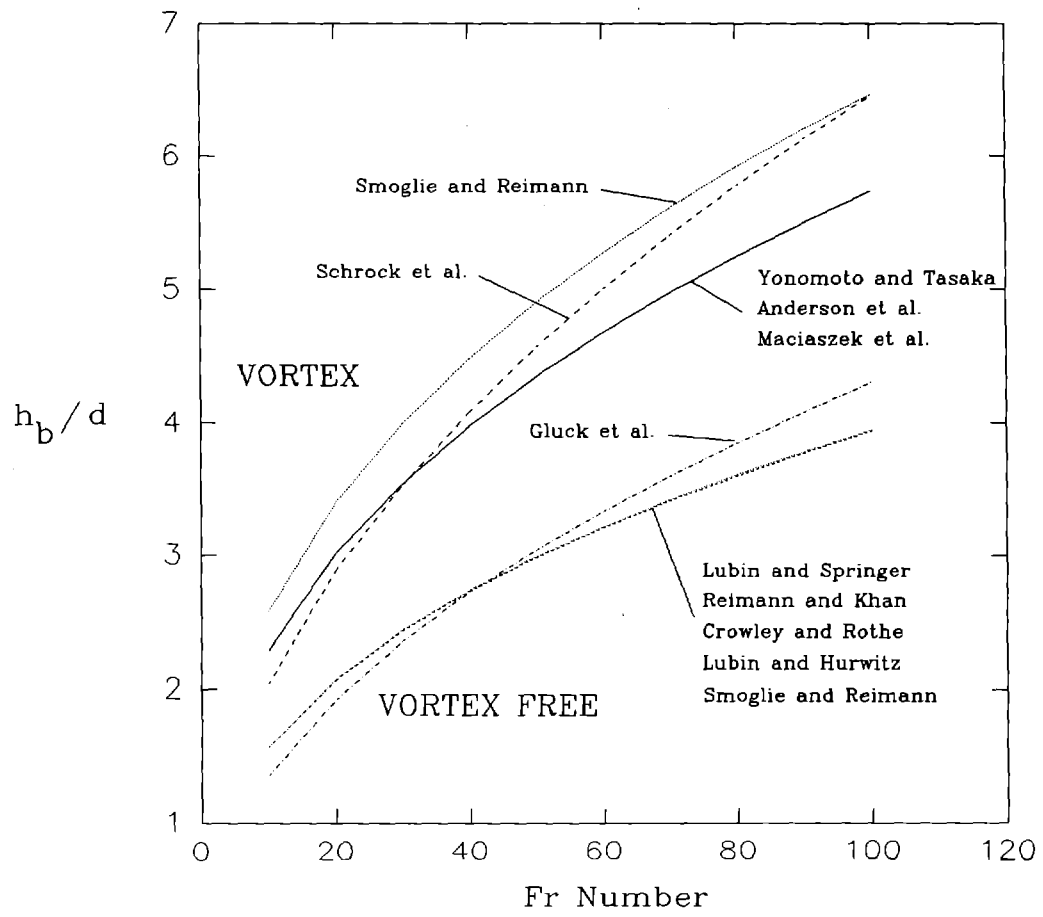


Figure 2. Correlation Comparison for the Onset of Gas Blowthrough

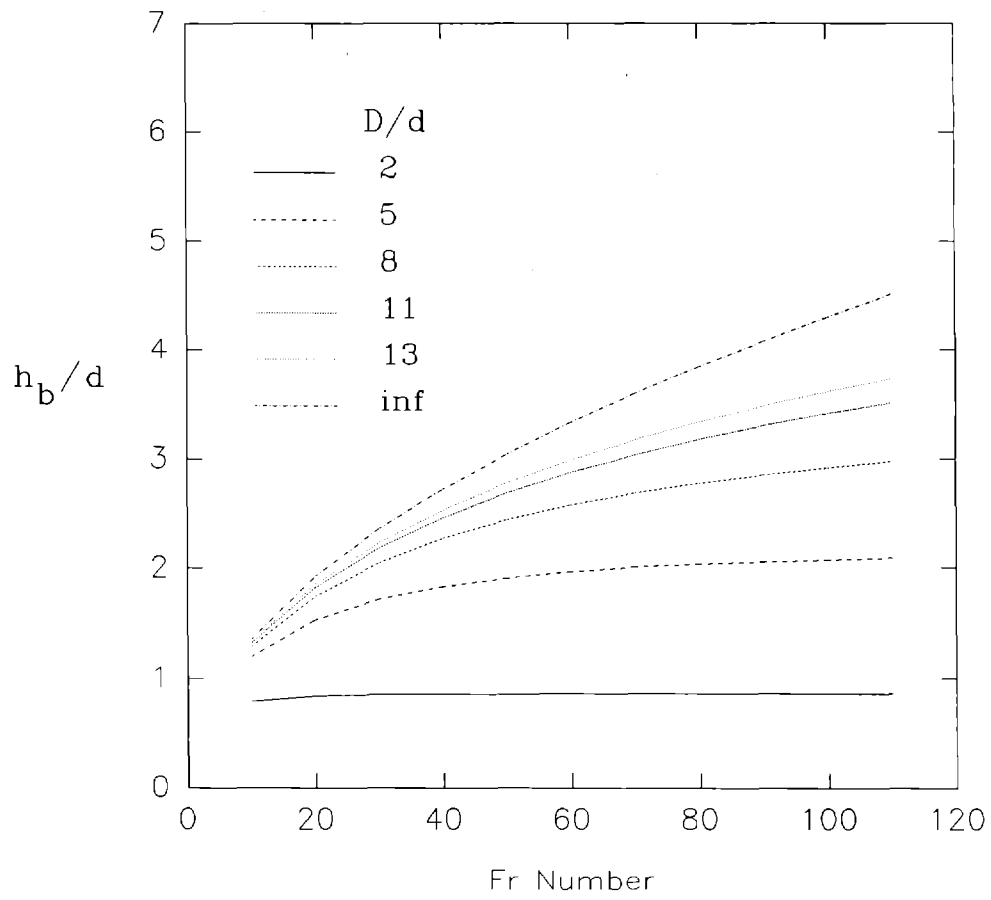


Figure 3. The Effect of Tank Diameter on the Onset of Gas Blowthrough

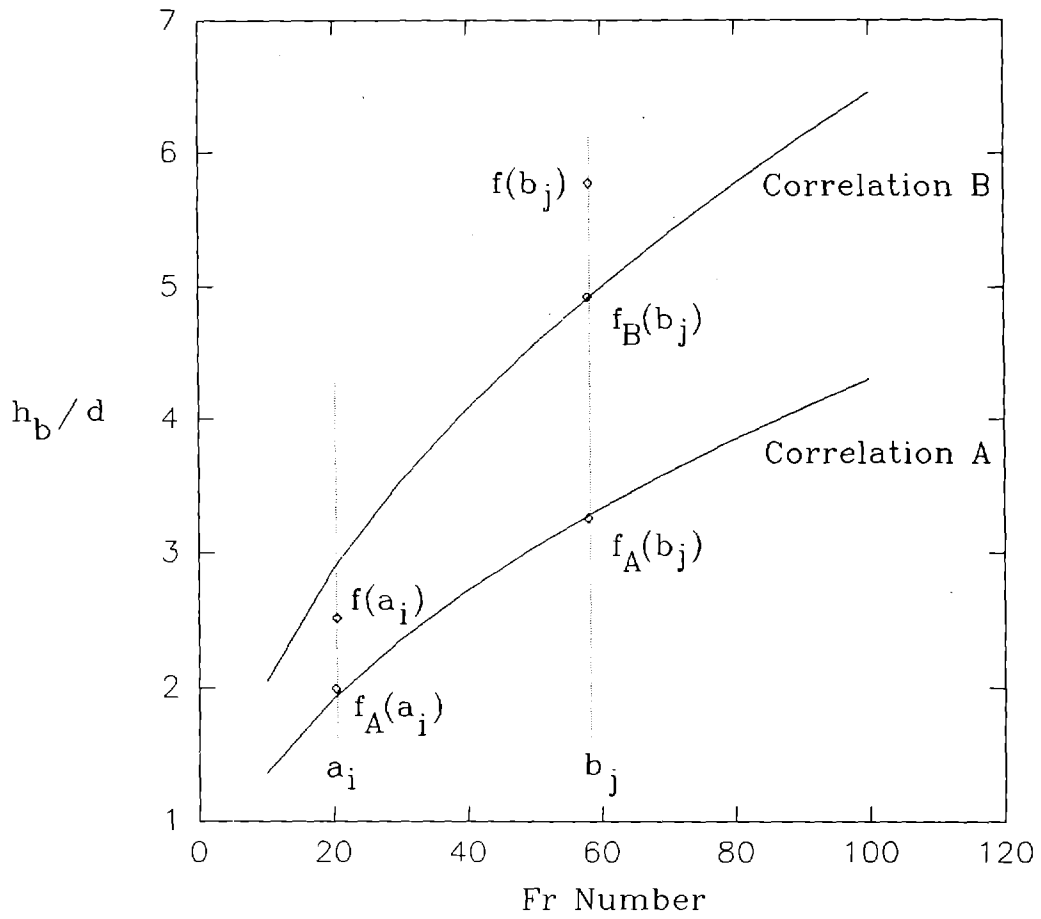


Figure 4. Contribution of Competitive Correlations to the Uncertainty in Applying a Recommended Correlation

3.0 FLOW QUALITY

Section 2.0 described the analysis of gas blowthrough as a process occurring during the first of three phases. The second of the three is a two-phase gas/liquid discharge. Two-phase discharge is initiated at the onset of gas blowthrough and continues until either the liquid or gas inventories are depleted. Two-phase discharge through a hole can be described in terms of either time-dependent void fractions or time dependent flow qualities.

The gas flow quality, X_g , is defined as the ratio of gas flow rate to total flow rate,

$$X_g = \frac{\dot{M}_g}{\dot{M}_g + \dot{M}_l} = \frac{1}{1 + \frac{\dot{M}_l}{\dot{M}_g}}, \quad (20)$$

where

\dot{M}_l, \dot{M}_g = liquid and gas mass flow rates respectively.

In an analogous fashion, the liquid flow quality can be defined such that

$$X_l + X_g = 1. \quad (21)$$

The gas flow quality is related to the void fraction by the identity

$$X_g = \frac{1}{1 + \frac{(1-\alpha_g) W_{sl}}{\alpha_g W_{sg}}} \quad (22)$$

which is obtained by the substitutions

$$\dot{M}_l = (1 - \alpha_g) W_{sl} \quad (23)$$

$$\dot{M}_g = \alpha_g W_{sg} \quad (24)$$

where

W_{sl}, W_{sg} = mass flow rates of liquid and gas respectively as if each phase flowed independently and completely filled the available flow area.

3.1 Scaling Analysis of Flow Quality

The gas flow quality is postulated to be a function of the following set of variables where two new variables,

$$X_g = f \{u; u_i; u_g; g; \rho_g; \rho_l; \mu_l; \sigma; h; d; D; \text{geometry}\} \quad (25)$$

u_g = velocity of gas out the hole, and
 h = instantaneous level of liquid above the hole,

have been added to the list from Equation 1. This list is thought to include all variables known or postulated by the relevant literature to influence flow quality. The implied assumption in formulating this list is that the flow quality is dominated by hydrodynamic phenomena that are not significantly influenced by the presence of solid particles, heat transfer, and chemical reactions. All these phenomena can exist to some degree in a reactor application; however, the authors have subjectively judged these concerns to be second order effects.

Application of the Buckingham Pi Theorem renders this set nondimensional,

$$X_g = f \left\{ \frac{h}{h_b}; Fr; Re; Bo; \frac{\rho_g}{\rho}; \frac{d}{D}; N_{Ti}; \frac{W_{sg}}{W_{sl}}; \text{geometry} \right\} . \quad (26)$$

The appearance of the blowthrough height (h_b) does not imply that it is an independent parameter that should have appeared in Equation 25 given above. The blowthrough height has the dependencies shown in Equation 2, all of which are already embodied in Equation 25 also given below; consequently, it is not an independent parameter. The use of h/h_b as a scaling group simply implies that there is a particularly useful combination of the groups listed in Equation 2. The utility of this selection is largely guided by the experience of experimenters; however, the model developed in Section 3.3 provides a technical basis for the importance of this scaling group.

A systematic reduction in the number of scaling groups performed for the onset of blowthrough is difficult to justify for flow quality. Table 5 summarizes the dependencies that appear in existing correlations. The ratio h/h_b is the common foundation for all the correlations. This ratio seems to completely capture the effect of the Froude number, which dominates correlations for the onset of blowthrough, attesting to the utility of h/h_b as a scaling group. Flow quality correlations show no dependence on the Reynolds number (viscosity) or the Bond number (surface tension), and this might be expected from the experience with blowthrough correlations. The density ratio does appear in some of the flow quality correlations in a fashion that is not totally negligible; this differs from prior experience with correlations for the onset of blowthrough. The effect of tank diameter has not been studied. Only two correlations show a dependence on gas flow rates, which seems a little odd because this term appears explicitly in the definitions of flow quality. All the available correlations are for horizontal pipes with downward-facing holes. Specific expressions for these correlations are summarized next.

3.2 Correlations for Flow Quality

Schrock et al. [1985] found that the gas exit quality could be expressed solely as a function of the depth ratio

$$X_g = (0.006)^{\frac{h}{h_b}} \left[1 - \frac{1}{2} \frac{h}{h_b} \left(1 + \frac{h}{h_b} \right) \right] \quad (27)$$

Schrock et al. [1986] recommended a different expression,

$$X_g = \left[1 - \left(\frac{h}{h_b} \right)^2 \right]^{3.5} \exp \left(-3.1 \frac{h}{h_b} \right) \quad (28)$$

in a later paper, but both the correlations are based substantially on the same data set. When evaluating this expression for flow quality, the appropriate expression for h_b (Equation 10 with constants C_1 and C_2 given in Table 2) that is consistent with the data base must be used.

Reimann and Khan [1983] developed a correlation for the liquid fraction at the orifice, which after substituting into Equation 22 yields

$$X_g = \frac{1}{1 + \frac{\left(\frac{h}{h_b} \right)^{1.62} \frac{W_{sl}}{W_{sg}}}{1 - \left(\frac{h}{h_b} \right)^{1.62}}} \quad (29)$$

for the gas flow quality. Using an expanded data set, Smoglie and Reimann [1986] later developed a more complicated expression for gas exit quality

$$X_g = \left[\frac{1.15}{1 + \left(\frac{\rho}{\rho_g} \right)^{0.5}} \right]^{\left(2.5 \frac{h}{h_b} \right)} \left[1 - \frac{1}{2} \frac{h}{h_b} \left(1 + \frac{h}{h_b} \right) \left(\frac{1.15}{1 + \left(\frac{\rho}{\rho_g} \right)^{0.5}} \right)^{\left(1 - \frac{h}{h_b} \right)} \right]^{0.5} \quad (30)$$

This expression is notable because of its explicit dependence on the density ratio. When evaluating this expression for flow quality, the appropriate expression for h_b (Equation 10 with constants C_1 and C_2 given in Table 2) that is consistent with the data base must be used.

Yonomoto and Tasaka [1988, 1991] start with the definition of gas quality (Equation 22) and computed the gas void fraction from the relations

$$\alpha_g = 0.9 \alpha_a \quad 0 < \alpha_a < 0.6 \quad (31)$$

$$\alpha_g = 1.15 \alpha_a - 0.15 \quad 0.6 < \alpha_a < 1.0 \quad (32)$$

$$\alpha_a = \frac{1 - B \left(\frac{h}{h_b} \right)^{2.5}}{2B} + \sqrt{\left[\frac{1 - B \left(\frac{h}{h_b} \right)^{2.5}}{2B} \right]^2 + \frac{1}{B} \left(\frac{h}{h_b} \right)^{2.5}} \quad (33)$$

$$B = \frac{W_{sg}}{W_{sl}} \sqrt{\frac{\rho_l}{\rho_g}} \quad (34)$$

where the flow rates are computed from

$$W_{sg} = C_d A_b \varepsilon \sqrt{2 \rho_g \Delta P} \quad (35)$$

$$W_{sl} = C_d A_b \sqrt{2 \rho \Delta P} \quad (36)$$

$$\varepsilon = 1 - 0.3707 \left[1 - \left(\frac{P_2}{P_1} \right)^{1/\gamma} \right]^{0.935} \quad (37)$$

When evaluating this expression for flow quality, the appropriate expression for h_b (Equation 10 with constants C_1 and C_2 given in Table 2) that is consistent with the data base must be used.

Geometry and tank diameter were found to be important factors influencing the onset of gas blowthrough, and it is reasonable to expect a similar importance in flow quality correlations. However, all of the quality correlations were developed for horizontal pipes, which is not the geometry of interest to experiment or NPP analyses of DCH events. Furthermore, tank diameter is not explicitly accounted for in any of the correlations. Consequently, none of the flow quality correlations is wholly suitable for DCH analyses, and there is a need for a more general correlation or model. The next section addresses this need.

3.3 Development of a Recommended Flow Quality Model for DCH Analyses

Pilch and Tarbell [1985] used the Gluck et al. [1966a,b] blowthrough correlation (which applies to the geometries of interest and accounts for the effects of tank diameter) as a seed for

a flow quality model. The derivation is repeated here because it has evolved somewhat from its first publication.

The development of the model proceeds as follows:

1. An upper bound for the void fraction, α_g , in the hole will be derived for hemispherical geometries.
2. The preceding step gives an upper bound for α_g only; therefore, a free parameter, N , will be introduced into the bounding expression.
3. The development in 1 and 2 will be repeated for horizontal pipe geometry.
4. The value of N will be chosen to match available experiment results for horizontal pipe geometry.
5. The same value of N will be applied to the model developed for hemispherical geometry.

The premise of the model is simple: at any instant, the liquid flow area through the hole must be sufficient to satisfy the blowthrough criteria at the current liquid depth. This follows from a one-to-one correspondence inherent in all the blowthrough correlations in which a critical depth for blowthrough is assigned to a specified liquid flow area characterized by a diameter, d_i . Alternatively, the blowthrough correlations can be viewed as assigning a critical liquid flow area to a specified depth, $A_{1,crit} = f(h)$. If the area of the hole is less than this critical value, then a surface disturbance will heal itself, blowthrough does not occur, and the liquid flow area is the total hole area. If, on the other hand, the area of the hole exceeds the critical liquid flow area, then blowthrough is expected, and the liquid flow area will be less than the hole area by an amount associated with the gas void,

$$\alpha_l A_b = (1 - \alpha_g) A_b \geq A_{1,crit} = f(h) \quad . \quad (38)$$

This places a lower bound on α_l (and an upper bound on α_g) if the physical state (or conceptual picture) of blowthrough is to be maintained.

This model requires that

$$h \leq 0.43D \tanh \left[\left(\frac{u}{\sqrt{gd_i}} \right)^{0.5} \frac{d_i}{D} \right] = 0.43D \tanh \left[Fr^{1/2} \frac{d}{D} \left(\frac{d_i}{d} \right)^{0.75} \right] , \quad (39)$$

be satisfied at every instant following blowthrough. Here, h ($h \leq h_b$) is the instantaneous depth of the liquid above the hole and d_i ($d_i \leq d$) is a dimension that characterized the fraction of the total flow area of the hole that is occupied by the liquid. The model provides a minimum liquid fraction for a specified depth. Dividing through by h_b and solving for d/d yields

$$\frac{d_i}{d} \geq \left(\frac{\operatorname{arctanh} \left[\frac{h}{h_b} \tanh \left(Fr^{0.5} \frac{d}{D} \right) \right]}{\frac{d}{D} Fr^{0.5}} \right)^{\frac{4}{3}} \quad (40)$$

It can be verified that this expression limits as expected; i.e., $d_i/d=1$ when $h/h_b=1$.

The term d_i/d is directly related to the liquid fraction at the hole. An obvious choice is

$$\frac{d_i}{d} = \left(\frac{A_l}{A_b} \right)^{1/2} = \alpha_l^{1/2} = (1 - \alpha_g)^{1/2} \quad (41)$$

which is independent of the morphology of the gas and liquid phases. Combining this result with Equation (40) yields

$$\alpha_l = \left(\frac{\operatorname{arctanh} \left[\frac{h}{h_b} \tanh \left(Fr^{0.5} \frac{d}{D} \right) \right]}{\frac{d}{D} Fr^{0.5}} \right)^{\frac{8}{3}} = \alpha_{l,\min} \quad (42)$$

for the minimum liquid fraction. The bounding nature of the formulation can be relaxed by introduction of an empirical exponent "N",

$$\alpha_l = \alpha_{l,\min}^N \quad (43)$$

which itself must be bounded by $0 < N < 1$. Justification for a recommended value of $N=0.6$ will be deferred for the moment. The best estimate gas void can then be expressed as

$$\alpha_g = 1 - \left(\frac{\operatorname{arctanh} \left[\frac{h}{h_b} \tanh \left(Fr^{0.5} \frac{d}{D} \right) \right]}{\frac{d}{D} Fr^{0.5}} \right)^{\frac{8N}{3}} \quad (44)$$

Upper bound or best estimate expressions (depending on the value of N) for the gas quality are obtained by combining Equation 43 with Equation 22. The flow rates can be computed from

$$W_{sg} = C_d A_b P_1 \left[\frac{MW_g}{R_u T} \left(\frac{2}{\gamma+1} \right)^{\frac{\gamma+1}{\gamma-1}} \right]^{\frac{1}{2}} \quad (45)$$

$$W_{sl} = C_d \rho_l A_b \left[\frac{2(P_1 - P_2)}{\rho_l} \right]^{\frac{1}{2}} \quad (46)$$

The first expression assumes separated isentropic choked flow of gas at the hole. For HPME events (i.e., $P_1 \gg P_2$ and $\gamma=1.3$) with equal gas and liquid discharge coefficients, the ratio of flow rates limits to a simple function of the density ratio,

$$\frac{W_{sl}}{W_{sg}} = 2.12 \sqrt{\frac{\rho_l}{\rho_g}} \quad (47)$$

This model cannot be tested directly because there is no flow quality data for hemispherical vessels or for vessels with a significant influence of tank diameter; however, the premise of the model can be tested by applying the same technique to blowthrough correlations that have been developed for horizontal cylinders. Applying the method outlined above to Equation 10 yields

$$\alpha_g = 1 - \left(\frac{h}{h_b} \right)^{\frac{4N}{2-C_2}} \quad (48)$$

For the commonly reported value $C_2=0.4$, this expression is identical to the correlation reported by Reimann and Khan [1983] when $N=0.648$.

Figure 5 confirms the bounding nature of the model developed here ($N=1.0$) for horizontal pipes (for conditions typical of the database). Note that the available correlations agree well with each other despite large variations for the onset of blowthrough (Figure 2). Excellent agreement with available correlations is obtained when $N=0.6$ is selected for the model developed here. This value is adopted for use in DCH analyses for hemispherical tanks of varying diameter. Clearly, there is a need for experiment data to confirm the modeling assumptions necessary to perform DCH analyses.

The recommended correlation for gas quality (Equations 44, 45 and 46 combined with Equation 22) is scale dependent because of the Froude number. Predicted flow qualities for typical experiment and NPP conditions (Table 6) are compared in Figure 6. Gas quality increases slightly with decreasing system scale.

Experience with the blowthrough correlation suggests that the gas quality is also dependent on the tank/hole diameter ratio. For NPP scale, Figure 7 shows that the gas quality

increases with decreasing tank/diameter ratios; however, the greater effect appears in the correlation for the onset of blowthrough (Figure 3).

3.4 Uncertainty in the Gas Quality Model

Direct assessment of the uncertainty associated with the gas quality model is not possible because there is no data for hemispherical systems or for systems with finite tank diameters. However, there is considerable experience with horizontal pipes, so it will be assumed that the uncertainty in gas quality correlations for pipes is indicative of gas quality correlations for hemispheres with finite tank diameters.

Table 7 summarizes the information necessary to estimate the total uncertainty in applying gas quality correlations to horizontal pipes. There are three independent data sets to choose from. All the data sets span the same range of parameters, so the data and correlation of Smoglie and Reimann is chosen as the recommended correlation because it lies between the other two correlations. Applying the techniques developed in Section 2.5, the overall uncertainty due to data scatter in the recommended correlation and existence of two competitive correlations is estimated to be $\pm 35\%$. Although quantified for horizontal pipes, this estimated uncertainty is assumed to be representative of what might be observed for hemispheres of finite diameter.

Table 5.
Scaling Dependencies for Available Flow Quality Correlations
with Downward Facing Holes

Reference	h/h_b	Fr	Re	Bo	ρ_g/ρ	d/D	W_{sg}/W_{sl}	Geometry
Schrock et al. 1985	X							Horizontal Pipe
Schrock et al. 1986	X							Horizontal Pipe
Riemann and Khan 1983	X						X	Horizontal Pipe
Smoglie and Riemann 1986	X				X			Horizontal Pipe
Yonomoto and Tasaka 1988	X				X		X	Horizontal Pipe

Table 6.
Parameters for Evaluating
the Gas Quality Correlation
for Hemispherical Tanks at Different Scales

Scale	h/h_b	D/d	Fr	ρ/ρ_g	P_1 (MPa)
NPP	0 - 1	10.0	12	284	6.28
Surtsey	0 - 1	11.4	54	162	6.28
ANL	0 - 1	11.4	108	162	6.28

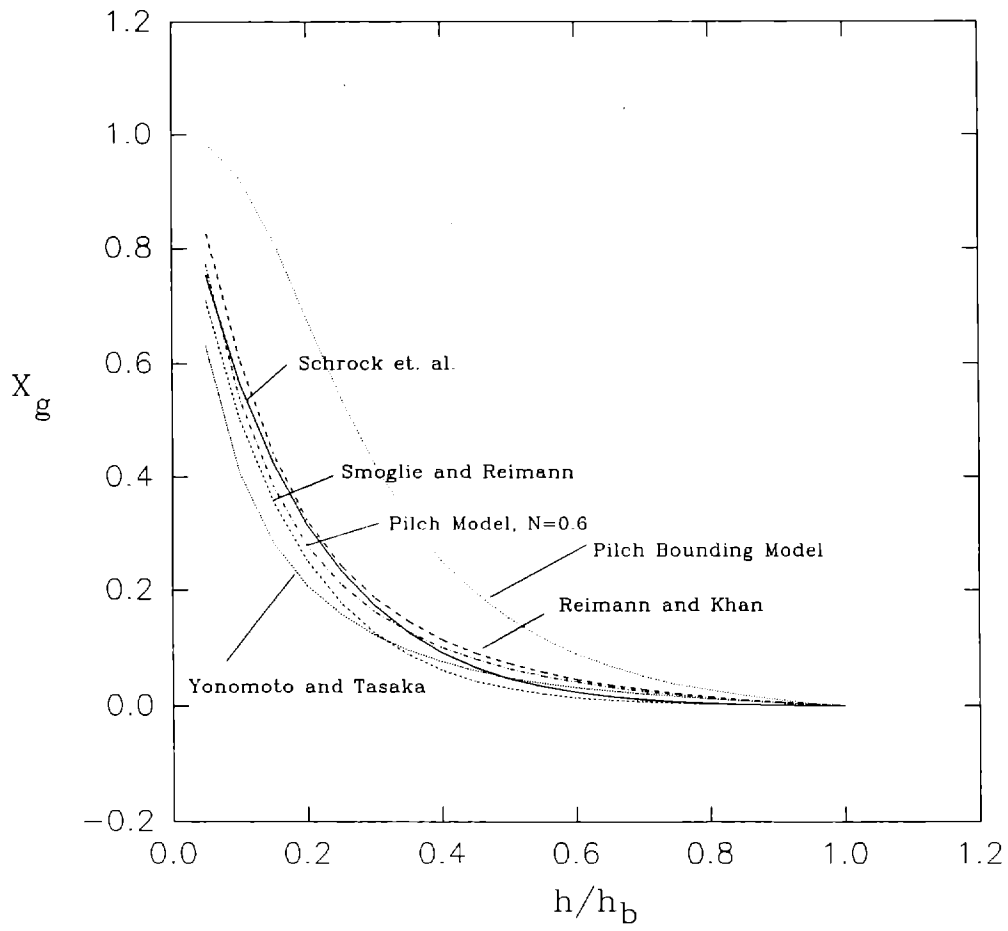


Figure 5. Model Comparison with Available Correlations Developed for Horizontal Pipes

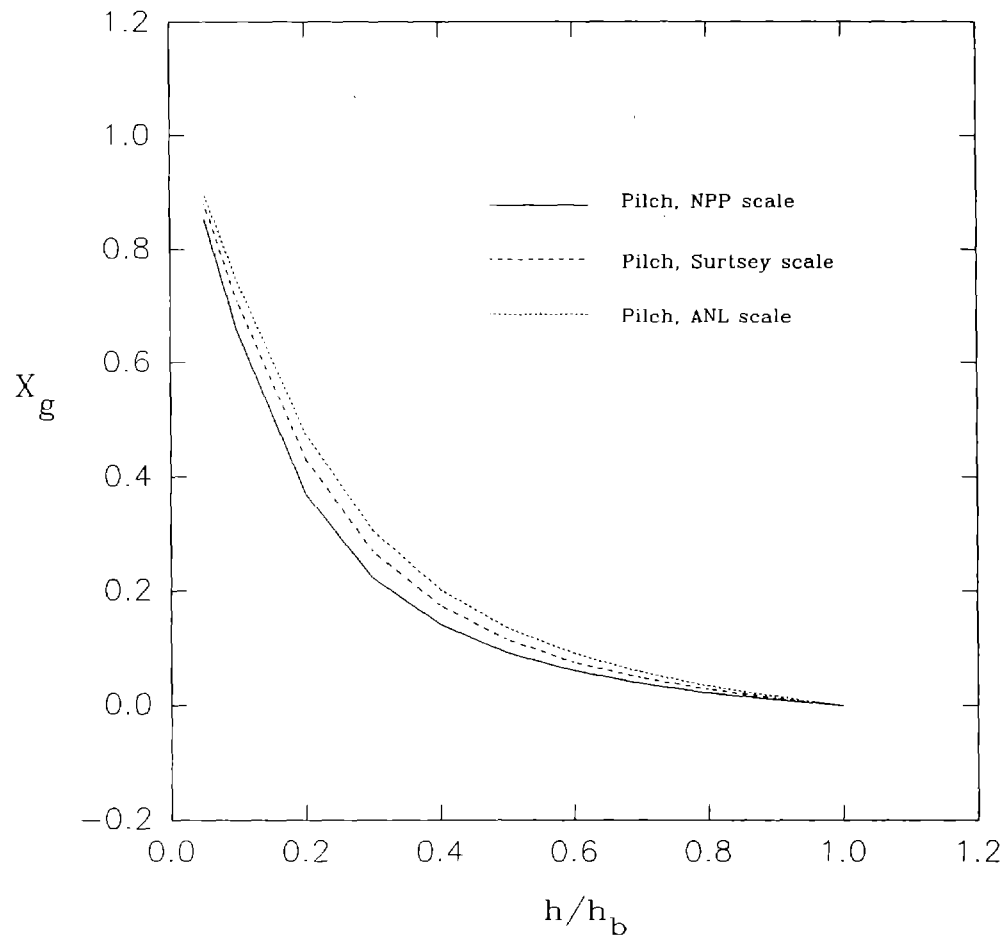


Figure 6. Predicted Effect of System Scale on Gas Quality

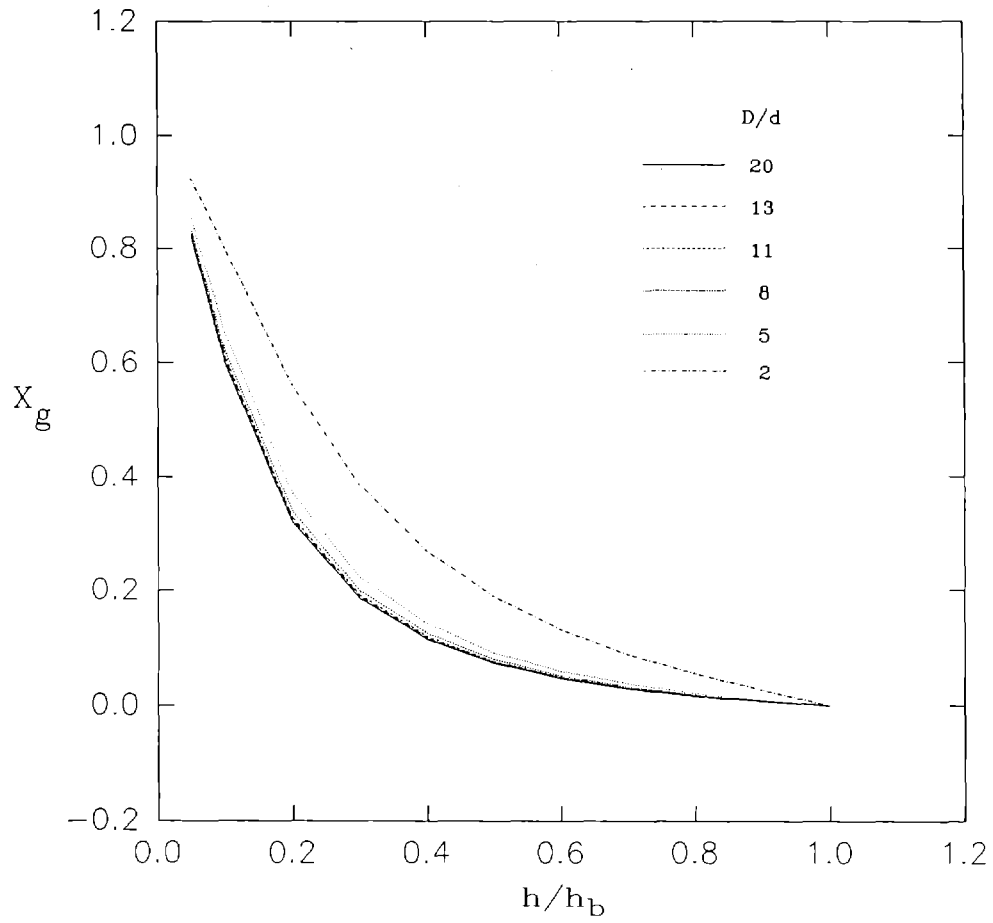


Figure 7. Predicted Effect of Tank/Hole Diameter Ratio at NPP Scale on Gas Quality

Table 7.
Parameters for Estimating the Overall Uncertainty
in Applying Gas Quality Correlations for Horizontal Pipes

Reference	N Data Points	σ RMS Scatter	δ RMS Offset
Smoglie and Riemann 1986	111	0.3	0
Schrock et al. 1986	59	0.3	0.25
Riemann and Khan 1983	19	0.3	0.40

4.0 CONCLUSIONS AND RECOMMENDATIONS

A number of correlations describing the advent of gas blowthrough and the subsequent exit quality were collected and examined. A simple scaling analysis was applied to these correlations to identify important nondimensional groups, and the range of values for these dimensionless groups at NPP and experimental scales was used to examine the applicability of the correlations at different scales. The performance of each of the correlations was also assessed over a typical parameter range for NPP and experimental conditions.

The Gluck et al. [1966a,b] correlation is recommended for use in analytical models of HPME at both NPP and experimental scales. The Gluck et al. [1966a,b] correlation is applicable to hemispherical geometry, and it is the only correlation that accounts for the effect of different tank sizes on gas blowthrough. Most importantly, it is also the only correlation developed over a wide enough range of parameters to fully encompass the expected conditions at NPP and experimental scales. The total expected uncertainty in the application of the Gluck et al. [1966a,b] correlation is estimated to be approximately $\pm 25\%$.

A new gas quality model was developed as part of this study. The new model is based on the Gluck et al. blowthrough correlation, and it is developed for the geometry of interest. Furthermore, it is the only correlation that accounts for the effects of tank diameter. The total expected uncertainty in the application of the new gas quality model is estimated to be approximately $\pm 35\%$.

The recommended correlations are judged to be the best models currently available for predicting gas blowthrough and exit quality in reactor systems. However, the lack of experiment data to assess the performance the gas quality model developed here represents a weakness in the model selection process. A separate effects experiment program designed to collect gas quality data over a wide range of Fr numbers and tank-to-hole diameter ratios in an upright hemispherical geometry would be invaluable in validating the model.

5.0 REFERENCES

- Allen, Michael D., Martin Pilch, Robert T. Nichols and Richard O. Griffith, Oct. 1991(a), Experiments to Investigate the Effect of Flight Path on Direct Containment Heating (DCH) in the Surtsey Test Facility: The Limited Flight Path (LFP) Tests, NUREG/CR-5728, SAND91-1105, Sandia National Laboratories, Albuquerque, NM.
- Allen, Michael D., Martin Pilch, Robert T. Nichols, John E. Brockmann, David W. Sweet and William W. Tarbell, Aug. 1991(b), Experimental Results of Direct Containment Heating by High-Pressure Melt Ejection into the Surtsey Vessel: The DCH-3 and DCH-4 Tests, SAND90-2138, Sandia National Laboratories, Albuquerque, NM.
- Allen Michael D., 1991(c), "The Integral Effects Test (IET-1) in the Surtsey Test Facility," SAND91-2613C, Proceedings of the Nineteenth Water Reactor Safety Information Meeting, Washington, D.C., Oct. 28-30.
- Allen, Michael D., Martin Pilch, Richard O. Griffith and Robert T. Nichols, 1992(a), Experiments to Investigate the Effect of Water in the Cavity on Direct Containment Heating (DCH) in the Surtsey Test Facility, SAND91-1173, Sandia National Laboratories, Albuquerque, NM.
- Allen Michael D., Martin Pilch, Richard O. Griffith and Robert T. Nichols, 1992(b), Experiments to Investigate the Effect of Ablated Hole Diameter on Direct Containment Heating (DCH) in the Surtsey Test Facility, 1992(b), SAND91-2153, Sandia National Laboratories, Albuquerque, NM.
- Allen Michael D., Martin Pilch, Richard O. Griffith, David C. Williams and Robert T. Nichols, 1992(c), The Third Integral Effects Test (IET-3) in the Surtsey Test Facility, SAND92-0166, Sandia National Laboratories, Albuquerque, NM.
- Anderson, J. L., and W. A. Owca, 1985, Data Report for the TPFL Tee/Critical Flow Experiments, NUREG/CR-4164, EGG-2377.
- Crowley, Christopher J., and Paul H. Rothe, 1981, "Flow Visualization and Break Mass Flow Measurements in Small Break Separate Effects Experiments," Small Break Loss-of-Coolant Accident Analyses in LWR's, Specialists Meeting, Aug. 25-27, Monterey, CA.
- Daggett, Larry L., and Garbis H. Keulegan, Nov. 1974, "Similitude in Free-Surface Vortex Formations," Journal of the Hydraulics Division, Proceedings of the ASCE, Vol. 100, No. HY11.
- Easton, C. R., and Ivan Catton, Dec. 1970, "Nonlinear Free Surface Effects in Tank Draining at Low Gravity," AIAA Journal, Vol. 8, No. 12.
- Gluck, D. F., J. P. Gille, D. J. Simkin and E. E. Zukoski, 1966a, "Distortion of the Liquid Surface During Tank Discharge Under Low G. Conditions," Aerospace Chemical Engineering No. 61, Vol 62.

- Gluck, D. F., J. P. Gille, E. E. Zukoski and D. J. Simkin, Nov. 1966b, "Distortion of a Free Interface During Tank Discharge," Journal of Spacecraft, Vol. 3, No. 11.
- Lubin, B., and M. Hurwitz, Oct. 1966, "Vapor Pull-Through at a Tank Drain - With and Without Dielectrophoretic Buffling," Proc. Conf. Long Term Cryo-Propellant Storage in Space, NASA Marshall Space Center, Huntsville, Ala., pg. 173.
- Lubin, Barry T., and George S. Springer, 1967, "The Formation of a Dip on the Surface of a Liquid Draining from a Tank," Journal of Fluid Mechanics, Vol. 29, part 2, pp. 385-390.
- Masiaszek, T., and A. Momponteil, 1986, "Experimental Study on Phase Separation in a Tee Junction for Steam Water Stratified Inlet Flow," European Two-Phase Flow Group Meeting, Munich, Germany.
- Murata, K. K., D. E. Carroll, K. E. Washington, F. Gelbard, G. D. Valdez, D. C. Williams and K. D. Bergeron, 1990, User's Manual for CONTAIN 1.1, A Computer Code for Severe Nuclear Reactor Accident Containment Analysis, NUREG/CR-5026, SAND87-2309, Sandia National Laboratories, Albuquerque, NM.
- NRC, Nov. 1991, An Integrated Structure and Scaling Methodology for Severe Accident Technical Issue Resolution, NUREG/CR-5809, EGG-2659.
- Pilch, M. and W. W. Tarbell, 1985, High Pressure Ejection of Melt from a Reactor Pressure Vessel - The Discharge Phase, NUREG/CR-4383, SAND85-0012, Sandia National Laboratories, Albuquerque, NM.
- Reimann, J., and M. Khan, 1983, "Flow Through a Small Break at the Bottom of a Large Pipe with Stratified Flow," Thermal Hydraulics of Nuclear Reactors, Vol. 1.
- Schrock, V. E., S. T. Revankar, R. Mannheimer and C-H Wang, 1985, Critical Flow Through a Small Break on a Large Pipe with Stratified Flow, NUREG/CP-0071, Transactions of the 13th Water Reactor Safety Research Information Meeting, Gaithersburg MA, October 22-25.
- Schrock, V. E., S. T. Revankar, R. Mannheimer, C-H Wang and D. Jia, Aug. 1986, "Steam-Water Critical Flow Through Small Pipes from Stratified Upstream Regions," 8th International Heat Transfer Conference, San Francisco, CA.
- Smoglie, C., and J. Reimann, 1986, "Two-Phase Flow Through Small Branches in a Horizontal Pipe with Stratified Flow," International Journal of Multiphase Flow, Vol. 12, No. 4, pp. 609-625.
- Smoglie, C., 1984, Two-Phase Flow Through Small Branches in a Horizontal Pipe with Stratified Flow, KfK-3861, Karlsruhe, Germany.

Williams, D. C., K. D. Bergeron, D. E. Carroll, R. D. Gasser, J. L. Tills, K. E. Washington, 1987, Containment Loads Due to Direct Containment Heating and Associated Hydrogen Behavior: Analysis and Calculations with the CONTAIN Code, NUREG/CR-4896, SAND87-0633, Sandia National Laboratories, Albuquerque, NM.

Williams, D. C., and D. L. Y. Louie, 1988, "CONTAIN Analyses of Direct Containment Heating Events in the Surry Plant," Proceedings of Thermal Hydraulics Division, ANS/ENS, Winter Meeting, Washington, D.C., Oct. 31-Nov. 4.

Yonomoto, T., and K. Tasaka, May 1988, "New Theoretical Model for Two-Phase Flow Discharged from Stratified Two-Phase Region through Small Break," Journal of Nuclear Science and Technology, 25, pp. 441-455, May 1988.

Yonomoto, T., and K. Tasaka, 1991, "Liquid and Gas Entrainment to a Small Break Hole from a Stratified Two-Phase Region," Int. J. Multiphase Flow, Vol. 17, No. 6, pp. 745-765.

DISTRIBUTION:

U. S. Nuclear Regulatory Commission (6)
Office of Nuclear Regulatory Research
Attn: C. Tinkler, NLN-344
A. Reuben, NLN-344
M. Cunningham, NLS-372
F. Eltawila, NLN-344
J. Mitchell, NLS-314
B. Sheron, NLS-007
Washington, D.C. 20555

U. S. Nuclear Regulatory Commission (3)
NRC/RES
Attn: E. Beckjord, NLS-007
B. Hardin, NLS-169
T. Speis, NLS-007
Washington, D.C. 20555

U. S. Department of Energy
Office of Nuclear Safety Coordination
Attn: R. W. Barber
Washington, D.C. 20545

U. S. Department of Energy (2)
Albuquerque Operations Office
Attn: C. E. Garcia, Director
For: C. B. Quinn
R. L. Holton
P. O. Box 5400
Albuquerque, NM 87185

Los Alamos National Laboratories
Attn: M. Stevenson
P.O. Box 1663
Los Alamos, NM 87545

W. Stratton
2 Acoma Lane
Los Alamos, NM 87544

Electric Power Research Institute (2)

Attn: A. Michiels
R. Sehgal
3412 Hillview Avenue
Palo Alto, CA 94303

R. Sherry
JAYCOR
P. O. Box 85154
San Diego, CA 92138

UCLA
Nuclear Energy Laboratory
Attn: I. Catton
405 Hilgaard Avenue
Los Angeles, CA 90024

Brookhaven National Laboratory (6)

Attn: R. A. Bari
T. Pratt
N. Tutu
130 BNL
Upton, NY 11973

Argonne National Laboratory (4)

Attn: J. Binder
C. Johnson
L. Baker, Jr.
B. Spencer
9700 S. Cass Avenue
Argonne, IL 60439

Fauske and Associates, Inc.

Attn: R. Henry
16W070 West 83rd Street
Burr Ridge, IL 60952

Battelle Columbus Laboratory (2)

Attn: R. Denning
J. Gieseke
505 King Avenue
Columbus, OH 43201

Department of Energy
Scientific and Tech. Info. Center
P. O. Box 62
Oak Ridge, TN 37831

University of Wisconsin
Nuclear Engineering Department
Attn: M. L. Corradini
1500 Johnson Drive
Madison, WI 53706

EG&G Idaho
Willow Creek Building, W-3
Attn: R. Hobbins
P. O. Box 1625
Idaho Falls, ID 83415

Battelle Pacific Northwest Laboratory
Attn: M. Freshley
P. O. Box 999
Richland, WA 99352

Professor Agustin Alonso
E.T.S. Ingenieros Industriales
Jost Gutierrez Abascal, 2
28006 Madrid
SPAIN

Jose Angel Martinez
Sub. Emplazamientos y Programas Coop.
CONSEJO DE SEGURIDAD NUCLEAR
Justo Dorado 11
28040 MADRID
SPAIN

Juan Bagues
Consejo de Seguridad Nuclear
SOR Angela de la Cruz No 3
Madrid 28056
SPAIN

Gesellschaft für Reaktorsicherheit (GRS)
Postfach 101650
Glockengrasse 2
5000 Köln 1
GERMANY

Technische Universität München
Attn: Professor H. Karwat
8046 Garching, Forschungsgelände
Munich
GERMANY

Siegfried Hagen
Kernforschungszentrum Karlsruhe
P.O. Box 3640
D-7500 Karlsruhe 1
GERMANY

Kernforschungszentrum Karlsruhe (2)
Attn: P. Hofmann
B. Kuczera
Postfach 3640
75 Karlsruhe
GERMANY

Klaus Trambauer
Gesellschaft für Reaktorsicherheit
Forschungsgelände
D-8046 Garching
GERMANY

UKAEA (3)
Attn: D. Sweet
S. Kinnersly 203/A32
D. Williams 210/A32
Winfrith, Dorchester
Dorset DT2 8DH
UNITED KINGDOM

UKAEA Culham Laboratory
Attn: B. D. Turland E5.157
Abingdon
Oxfordshire OX14 3DB
UNITED KINGDOM

UKAEA
Reactor Development Division
Attn: T. Butland
Winfrith, Dorchester
Dorset DT2 8DH
UNITED KINGDOM

M. R. Hayns
AEA Reactor Services
B329
Harwell
Didcot
Oxfordshire OX11 0RA
UNITED KINGDOM

Mr. F. Abbey (2)
AEA Technology
Safety and Reliability Directorate
Wigshaw Lane
Culcheth
Cheshire WA3 4NE
UNITED KINGDOM

Simon J. Board
CEGB National Power
Barnett Way
Barnwood, Gloucestershire GL4 7RS
ENGLAND

Nigel E. Buttery
Central Elect. Gen. Board, Booths Hall
Chelford Road, Knutsford
Cheshire WA16 8QG
ENGLAND

Nucleare e della Protezione Sanitaria (DISP)
Attn: Mr. G. Petrangeli
Ente Nazionnle Energie Alternative (ENEA)
Viale Regina Margherita, 125
Casella Postale M. 2358
I-00100 Roma A. D.
ITALY

G. Caropreso
Dept. for Environmtl Protection & Health
ENEA CRE Casaccia
Via Anguillarese, 301
00100 Roma Ad.
ITALY

P. Ficara
Department for Thermal Reactors
ENEA CRE Casaccia
Via Anguillarese, 301
00100 Roma Ad.
ITALY

Alan V. Jones
Thermodynamics & Rad. Physics, TP-650
CEC Joint Research Center, Ispra
I-21020 Ispra (Varese)
ITALY

Dr. K. J. Brinkman
Reactor Centrum Nederland
1755 ZG Petten
THE NETHERLANDS

Mr. H. Bairiot, Chief
Department LWR Fuel
Belgonucleaire
Rue de Champde Mars. 25
B-1050 Brussels
BELGIUM

Japan Atomic Energy Research Institute
Attn: K. Sato
Fukoku Seimei Bldg.
2-2-2, Uchisaiwai-cho, Chiyoda-ku, Tokyo
100
JAPAN

Japan Atomic Energy Institute
Severe Accident Research Laboratory
Attn: Dr. K. Soda, Head
Tokai-mura, Naka-gun, Ibaraki-ken
319-11
JAPAN

Japan Atomic Energy Research Institute
Reactivity Accident Laboratory
Attn: Toyoshi Fuketa
Tokai-Mura, Ibaraki-Ken
319-11
JAPAN

R. D. MacDonald
Atomic Energy Canada, Ltd.
Chalk River, Ontario
CANADA KOJ IJO

Atomic Energy Canada Ltd.
Attn: Vijay I. Ngth
Sheridan Park Res. Comm.
Mississauga, Ontario
CANADA L5K 1B2

Oguz Akalin
Ontario Hydro
700 University Avenue
Toronto, Ontario
CANADA M5G 1X6

K. N. (Kannan) Tennankore
Safety Research Division
Whiteshell Nuclear Res. Establishment
Pinawa, Manitoba
CANADA ROE 1LO

J. Clive Wood
Safety Research Division
Whiteshell Nuclear Res. Establishment
Pinawa, Manitoba
CANADA ROE 1LO

M. Jankowski
IAEA
Division of Nuclear Reactor Safety
Wagranesrstrasse 5
P. O. Box 100
A/1400 Vienna
AUSTRIA

Statens Kernkraftinspektion (2)
Attn: L. Hammer
W. Frid
P. O. Box 27106
S-10252 Stockholm
SWEDEN

Studvik Energiteknik AB
Attn: K. Johansson
S-611 82 Nykoping
SWEDEN

Korea Adv Energy Research Inst
Attn: Hee-Dong Kim
P. O. Box 7
Daeduk-Danji
Choong-Nam
KOREA

Chang K. Park
Korea Atomic Energy Research Institute
Korea Advanced Energy Research Institute
P.O. Box 7, Daeduk Danji
Taejon 305-353
KOREA

Jong In Lee
Severe Accident Assessment Department
Korea Institute of Nuclear Safety
P.O. Box 16, Daeduk-Danji
Daejeon, 305-353
KOREA

POSTECH
Department of Mechanical Engineering
Attn: Moo Hwan Kim
P. O. Box 125
Kyungbuk 790-600
KOREA

Institute of Nuclear Energy Research
Attn: Yi-Bin Chen
P. O. Box 3
Lungtan
Taiwan 32500
REPUBLIC OF CHINA

Ms. C. Lecomte
CEN FAR
60-68 Av. du G. Leclerc - B.P.6
92265 Fontenay aux Roses cedex
FRANCE

Dr. A. Meyer-Heine
CEN Cadarache
13108 Saint Paul lez Durance
FRANCE

Dr. A. Tattegrain
CEN Cadarache
13108 Saint Paul lez Durance
FRANCE

Dr. G. Hache
CEN Cadarache
13108 Saint Paul lez Durance
FRANCE

Jacques Duco
Centre d'Etudes Nucleaires (IPSN-DAS)
Commissariat a l'Energie Atomique
Boite Postale No. 6
F-92265 Fontenay-aux-Roses Cedex
FRANCE

Maurice Gomolinski
Protection and Nuclear Safety Institute
Commissariat a l'Energie Atomique
Boite Postale No. 6
F-92265 Fontenay-aux-Roses Cedex
FRANCE

Michel Livolant
Inst. de Protection et de Surete Nucl.
Commissariat a l'Energie Atomique
Boite Postale No. 6
F-92265 Fontenay-aux-Roses Cedex
FRANCE

Jorma V. Sandberg
Department of Nuclear Safety
Finnish Center Radiation & Nucl. Safety
P.O. Box 268
SF-00101 Helsinki
FINLAND

Lasse Mattila
Nuclear Engineering Laboratory
Technical Research Center of Finland
P.O. Box 169
SF-00181 Helsinki
FINLAND

S. Chakraborty
Swiss Federal Nucl. Safety Inspectorate
CH-5303 Wurenlingen
SWITZERLAND

J. Peter Hosemann
Light Water Reactor Safety Program
Paul Scherrer Institute
CH-5232 Villigen PSI
SWITZERLAND

Vladimir Asmolov
I.V. Kurchatov Institute of Atomic Energy
Moscow 123182
Kurchatov Square
USSR

1810 D. W. Schaeffer
7141 S. A. Landenberger (5)
7613-2 Document Processing for DOE-OSTI (8)
7151 G. C. Claycomb (3)
6321 B. D. Zak
6400 N. R. Ortiz
6405 D. A. Dahlgren
6412 A. L. Camp
6415 S. L. Thompson
6418 R. K. Cole
6414 J. E. Kelly
6404 D. A. Powers (2)
6422 M. D. Allen (5)
6422 T. K. Blanchat (5)
6422 J. E. Brockmann
6422 E. R. Copus
6422 M. Pilch (5)
6422 R. T. Nichols
6422 P. Guyer (10)
6423 K. O. Reil
6429 K. E. Washington
6429 R. O. Griffith
6429 D. C. Williams
6403 W. A. Von Rieseemann
8523-2 Central Technical Files